16.485: Visual Navigation for Autonomous Vehicles (VNAV) **Fall 2020**

Lecture 4

Lecturer: Luca Carlone *Scribes: -*

This lecture reviews geometric concepts introduced in Lectures 2-3 in terms of differential geometry and Lie Groups. In particular, we will cover:

- basic concepts about Lie Groups
- Exponential and Logarithm maps
- distances between group elements

Why do we need to review the concepts from Lecture 2 in a group-theoretic perspective? Because the Lie group perspective allows for a unified treatment of rotations and poses (e.g., useful later on when we discuss optimization on-manifold), and to introduce the notion of "distance" between poses and between rotations in a more formal manner.

An introductory reference for this is [1, p. 205-256].

4.1 Groups and Lie Groups

A *group* $\mathcal{G}$ is a (finite or infinite) set of elements together with a binary *group operation* $\otimes$ that satisfies the following conditions:

- *closure*: for any $A, B \in \mathcal{G}$, it holds $A \otimes B \in \mathcal{G}$
- *associativity*: for any $A, B, C \in \mathcal{G}$, it holds $(A \otimes B) \otimes C = A \otimes (B \otimes C)$
- *identity element*: there exists an identity element $I \in \mathcal{G}$ such that $A \otimes I = I \otimes A = A$ for any $A \in \mathcal{G}$
- *inverse*: for any $A \in \mathcal{G}$ there exist an inverse element A^{-1} such that $A \otimes A^{-1} = A^{-1} \otimes A = I$

Note that the notion of *vector space* is much stronger than the notion of group, since a vector space has two operations (addition and multiplication by scalar) and satisfies a large set of *axioms* (associativity of addition, commutativity of addition, identity element of addition, inverse element of addition, and other properties regarding the scalar product).

Example 4.1.1 (General Linear Group $\mathrm{GL}(d, \mathbb{R})$)**.** Set of invertible $\mathbb{R}^{d \times d}$ matrix with matrix multiplication as group operation.

The following are groups of interest for VNAV, all using the matrix multiplication as group operation.

Example 4.1.2 (Orthogonal Group $\mathrm{O}(d)$)**.** The group of orthogonal matrices $\mathrm{O}(d) \doteq \left\{ \boldsymbol{R} \in \mathbb{R}^{d \times d} \ : \ \boldsymbol{R}^{\mathsf{T}} \boldsymbol{R} = \mathbf{I}_d \right\}$. Note: an orthogonal matrix can only have determinant $+1$ or -1.

Example 4.1.3 (Special Orthogonal Group SO(d))**.** The group of rotation matrices - it is the subset of $d \times d$ matrices defined as $\mathrm{SO}(d) \doteq \left\{ \boldsymbol{R} \in \mathbb{R}^{d \times d} \,:\, \boldsymbol{R}^\mathsf{T}\boldsymbol{R} = \mathbf{I}_d, \det(\boldsymbol{R}) = +1 \right\}$. This is sometimes called the group of *proper rotations*. Note that $\mathrm{SO}(d) \subset \mathrm{O}(d)$ since $\mathrm{O}(d)$ also includes orthogonal matrices with determinant -1 that represent *improper rotations* or *reflections* (also: left-handed coordinate frames).

Example 4.1.4 (Special Euclidean Group SE(d))**.** The group of $(d+1) \times (d+1)$ matrices representing rigid transformations, i.e., poses expressed in homogeneous coordinates.

In general, all the groups above are *non-abelian* (i.e., the group operation is not commutative).

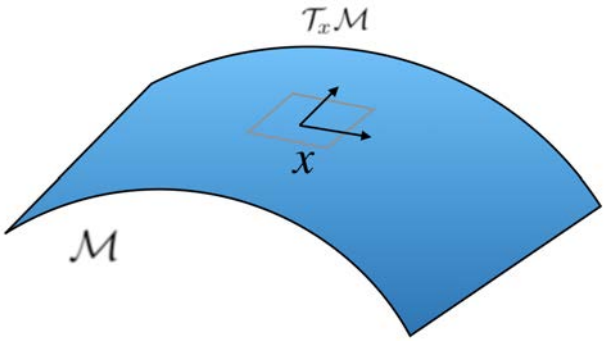

Figure 4.1: 2-dimensional manifold embedded in 3D space and tangent space at x.

Manifold. An *d-dimensional manifold* $\mathcal{M}$ is a topological space where the neighborhood of every point $x \in \mathcal{M}$ is homeomorphic to $\mathbb{R}^d$. Informally: a low-dimensional surface embedded in a higher-dimensional space which looks "flat" at any point.

Tangent space: A d-dimensional manifold $\mathcal{M}$ embedded has a *tangent space* for every point $x \in \mathcal{M}$. The tangent space at x is denoted as $\mathcal{T}_x\mathcal{M}$ and has dimension d.

Chart & Atlas: invertible map between a subset of a d-dimensional topological manifold and a subset of the Euclidean space $\mathbb{R}^d$. A chart is a local "map" and the collection of charts covering the entire manifold is called an *atlas*.

Differentiable manifolds: a manifold where we can move from one chart to another using a differentiable function (the *transition map*). If the transition map is smooth (infinitely differentiable), the manifold is called a *smooth manifold*.

Riemannian manifold: A smooth manifold equipped with a notion of distance (the *Riemannian distance*) given by a smooth positive definite symmetric bilinear metric defined on the tangent space at each point. Riemannian manifolds allow generalizing the intuitive notion of Euclidean distance to "curved surfaces": while the minimum-distance path between two points in Euclidean space is a straight line, the minimum-distance path on a Riemannian manifold is a *geodesic*, i.e., the shortest continuous curve connecting the two points on the manifold.

Lie Groups. A group is said to be a *Lie group* embedded in $\mathbb{R}^N$ if:

- $\mathcal{G}$ is a manifold in $\mathbb{R}^N$.
- the group operations (composition and inverse) are smooth (infinitely differentiable).

Example 4.1.5 (Rotations and poses)**.** $\mathrm{SO}(d)$, $\mathrm{O}(d)$, $\mathrm{SE}(d)$ are *matrix Lie groups*.

4.2 Lie algebras

Every matrix Lie group is associated a *Lie algebra*, which consists of a vector space, called the *tangent space*, and a binary operation called the *Lie Bracket*. For the moment, we will not worry about defining the Lie Bracket, but we focus on the tangent space. The interested reader can find the definition of the Lie Bracket operation for different matrix groups in [1, Section 6].

Example 4.2.1 (Lie algebra of SO(3))**.** The vector space corresponding to the Lie algebra of SO(3) is:

$$\mathrm{so}(3) = \left\{ \begin{bmatrix} 0 & -\phi_3 & \phi_2 \\ \phi_3 & 0 & -\phi_1 \\ -\phi_2 & \phi_1 & 0 \end{bmatrix} \; : \; \boldsymbol{\phi} = [\phi_1 \; \phi_2 \; \phi_3]^\mathsf{T} \in \mathbb{R}^3 \right\} \tag{4.1}$$

which corresponds to the set of skew-symmetric matrix in $\mathbb{R}^{3\times 3}$.

For notational convenience we define the *hat* $(\cdot)^\wedge$ and the *vee* $(\cdot)^\vee$ operators as follows:

$$(\boldsymbol{\phi})^\wedge \doteq \begin{bmatrix} 0 & -\phi_3 & \phi_2 \\ \phi_3 & 0 & -\phi_1 \\ -\phi_2 & \phi_1 & 0 \end{bmatrix} \text{ and } \begin{bmatrix} 0 & -\phi_3 & \phi_2 \\ \phi_3 & 0 & -\phi_1 \\ -\phi_2 & \phi_1 & 0 \end{bmatrix}^\vee \doteq \boldsymbol{\phi} \tag{4.2}$$

Example 4.2.2 (Lie algebra of SE(3))**.** The vector space corresponding to the Lie algebra of SE(3) is:

$$\mathrm{se}(3) = \left\{ \begin{bmatrix} \boldsymbol{\phi}^\wedge & \boldsymbol{\rho} \\ \mathbf{0}_3^\mathsf{T} & 0 \end{bmatrix} \; : \; \boldsymbol{\rho}, \boldsymbol{\phi} \in \mathbb{R}^3 \right\} \tag{4.3}$$

For notational convenience we "overload" the *hat* $(\cdot)^\wedge$ and the *vee* $(\cdot)^\vee$ operators to work on vectors $\xi \in \mathbb{R}^6$ as vectors:

$$\xi^\wedge = \begin{bmatrix} \boldsymbol{\phi} \\ \boldsymbol{\rho} \end{bmatrix}^\wedge \doteq \begin{bmatrix} \boldsymbol{\phi}^\wedge & \boldsymbol{\rho} \\ \mathbf{0}_3^\mathsf{T} & 0 \end{bmatrix} \quad \text{and} \quad \begin{bmatrix} \boldsymbol{\phi}^\wedge & \boldsymbol{\rho} \\ \mathbf{0}_3^\mathsf{T} & 0 \end{bmatrix}^\vee \doteq \xi = \begin{bmatrix} \boldsymbol{\phi} \\ \boldsymbol{\rho} \end{bmatrix} \tag{4.4}$$

The matrix $\xi^\wedge$ is also called a "screw" matrix [7].

4.3 Exponential and Logarithm map

The *exponential map* and the *logarithm map* relate elements of a matrix Lie group with elements in the corresponding Lie algebra. In particular, the *exponential map* produces a matrix Lie group element $\boldsymbol{G}$ from a Lie algebra element $\boldsymbol{A} \doteq \boldsymbol{a}^\wedge$ via a matrix exponential:

$$\boldsymbol{G} = \exp(\boldsymbol{A}) = \sum_{n=0}^{\infty} \frac{1}{n!} \boldsymbol{A}^n \tag{4.5}$$

Similarly, the *logarithm map* produces a Lie algebra element $\boldsymbol{A}$ from a matrix Lie group element $\boldsymbol{G}$ via a matrix logarithm:

$$\boldsymbol{A} = \log(\boldsymbol{G}) = \sum_{n=1}^{\infty} \frac{(-1)^{n-1}}{n} (\boldsymbol{G} - \mathbf{I})^n \tag{4.6}$$

Example 4.3.1 (Exponential and Logarithm maps for SO(3))**.** Any element of so(3) is a 3×3 skew symmetric matrix, and this allows simplifying the expression of the exponential map for SO(3), which can be written in closed-form as follows:

$$\boldsymbol{R} = \exp(\boldsymbol{\phi}^\wedge) = \cos(\|\boldsymbol{\phi}\|)\mathbf{I}_3 + \sin(\|\boldsymbol{\phi}\|) \left[\frac{\boldsymbol{\phi}}{\|\boldsymbol{\phi}\|} \right]_\times + (1 - \cos(\|\boldsymbol{\phi}\|)) \left(\frac{\boldsymbol{\phi}}{\|\boldsymbol{\phi}\|} \right) \left(\frac{\boldsymbol{\phi}}{\|\boldsymbol{\phi}\|} \right)^\mathsf{T} \tag{4.7}$$

Now we observe that the expression above resembles the Rodrigues' rotation formula. Indeed, if we interpret $\theta \doteq \|\boldsymbol{\phi}\|$ as a rotation angle and $\boldsymbol{u} \doteq \frac{\boldsymbol{\phi}}{\|\boldsymbol{\phi}\|}$ as a rotation axis (a unit vector) the expression above is identical to the Rodrigues' rotation formula, suggesting that vectors in the tangent space are in the form

$$\boldsymbol{\phi} = \theta \boldsymbol{u} \tag{4.8}$$

In hindsight, we found a new rotation parametrization. We will refer to $\boldsymbol{\phi}$ as the *exponential coordinates* of the rotation. The vector $\boldsymbol{\phi}$ is also called a *rotation vector* or *Euler vector*.

Example 4.3.2 (Exponential and Logarithm maps for SE(3))**.** Using the special structure of the 4×4 skew matrix in se(3), we can simplify the expression of the exponential map for SE(3), which can be written in closed-form as follows:

$$\boldsymbol{T} = \exp(\boldsymbol{\xi}^\wedge) = \exp\left(\begin{bmatrix} \boldsymbol{\phi} \\ \boldsymbol{\rho} \end{bmatrix}^\wedge\right) = \begin{bmatrix} \exp(\boldsymbol{\phi}^\wedge) & \boldsymbol{J}_l(\boldsymbol{\phi})\boldsymbol{\rho} \\ \mathbf{0}_3^\intercal & 1 \end{bmatrix} \tag{4.9}$$

where $\boldsymbol{J}_l(\phi)$ is called the *left-jacobian* (for SO(3)) and has the following expression:

$$\boldsymbol{J}_l(\boldsymbol{\phi}) \doteq \mathbf{I}_3 + \frac{1-\cos(\|\boldsymbol{\phi}\|)}{\|\boldsymbol{\phi}\|^2}\boldsymbol{\phi}^\wedge + \frac{\|\boldsymbol{\phi}\| - \sin(\|\boldsymbol{\phi}\|)}{\|\boldsymbol{\phi}\|^3}\boldsymbol{\phi}^\wedge\boldsymbol{\phi}^\wedge \tag{4.10}$$

The logarithm map can be also computed in closed-form:

$$\xi^\wedge = \begin{bmatrix} \boldsymbol{\phi} \\ \boldsymbol{\rho} \end{bmatrix}^\wedge = \log\left(\begin{bmatrix} \boldsymbol{R} & \boldsymbol{t} \\ \mathbf{0}_3^\intercal & 1 \end{bmatrix}\right) = \begin{bmatrix} \boldsymbol{\phi} \\ \boldsymbol{J}_l^{-1}(\boldsymbol{\phi})\boldsymbol{t} \end{bmatrix}^\wedge \tag{4.11}$$

where $\boldsymbol{\phi} = \log(\boldsymbol{R})^\vee$. Again, the inverse of the left Jacobian can be expressed in closed-form as:

$$\boldsymbol{J}_l^{-1}(\boldsymbol{\phi}) \doteq \mathbf{I}_3 - \frac{1}{2}\boldsymbol{\phi}^\wedge + \left(\frac{1}{\|\boldsymbol{\phi}\|^2} - \frac{1+\cos(\|\boldsymbol{\phi}\|)}{2\|\boldsymbol{\phi}\|\sin(\|\boldsymbol{\phi}\|)}\right)\boldsymbol{\phi}^\wedge\boldsymbol{\phi}^\wedge \tag{4.12}$$

Derivations for these matrices (and more) are given around page 40 of [4].

The exponential maps for SO(3) and SE(3) are surjective-only in the sense that there exist many Lie algebra elements that produce the same Lie group element.

4.4 Distances

In many applications, one needs to quantify how "different" two rotations or poses are. For this purpose, we need the notion of distance.

4.4.1 Distances between rotations

There are multiple possible definitions of what a distance between two rotations is. The choice of distance is often dictated by analytical and computational convenience. An excellent review of these metrics is given in [6]. We review these distance metrics below.

Before delving into details, we recall that a "metric" (or distance) $\mathbf{dist}(a, b)$ between two generic elements "a" and "b" satisfies the following properties:

$$\mathbf{dist}(a,b) \geq 0 \qquad \text{(non-negativity)} \tag{4.13}$$

$$\mathbf{dist}(a,b) = 0 \iff a = b \qquad \text{(identity)} \tag{4.14}$$

$$\mathbf{dist}(a,b) = \mathbf{dist}(b,a) \qquad \text{(symmetry)} \tag{4.15}$$

$$\mathbf{dist}(a,c) \leq \mathbf{dist}(a,b) + \mathbf{dist}(b,c) \qquad \text{(triangle inequality)} \tag{4.16}$$

4.4.2 Angular (or geodesic) distance in SO(3)

A fairly intuitive metric for the distance between two rotations $\boldsymbol{R}_A \in \mathrm{SO}(3)$ and $\boldsymbol{R}_B \in \mathrm{SO}(3)$ can be obtained by (i) computing the relative rotation $\boldsymbol{R}_{AB} = \boldsymbol{R}_A^\mathsf{T}\boldsymbol{R}_B$ and (ii) computing the rotation angle θ_{AB} of the rotation $\boldsymbol{R}_{AB}$ (as in the axis-angle representation), (iii) taking the absolute value of the rotation angle (unless we restrict $\theta \in [0, \pi) \ldots$). Intuitively, this is the rotation angle (around some axis) that can align $\boldsymbol{R}_A$ to $\boldsymbol{R}_B$. Such a metric, is called the *angular distance*, and, using the formula to compute the rotation angle from a rotation matrix we saw in the previous lecture, we write this metric as:

$$\mathbf{dist}_\theta(\boldsymbol{R}_A, \boldsymbol{R}_B) = \left| \arccos\left(\frac{\mathrm{tr}\left(\boldsymbol{R}_A^\mathsf{T}\boldsymbol{R}_B\right) - 1}{2} \right) \right| \tag{4.17}$$

Recalling that the norm of the exponential coordinates is the rotation angle, the previous metric can be written as:

$$\mathbf{dist}_\theta(\boldsymbol{R}_A, \boldsymbol{R}_B) = \| \log(\boldsymbol{R}_A^\mathsf{T}\boldsymbol{R}_B)^\vee \| = \| \log(\boldsymbol{R}_B^\mathsf{T}\boldsymbol{R}_A)^\vee \| \tag{4.18}$$

It can be shown that this distance is a *geodesic* distance, i.e., it is the length of the minimum path between $\boldsymbol{R}_A$ and $\boldsymbol{R}_B$ on the manifold SO(3).

Bi-invariance: for 3 rotations $\boldsymbol{R}_A, \boldsymbol{R}_B, \boldsymbol{R}_C$:

$$\mathbf{dist}_\theta(\boldsymbol{R}_A, \boldsymbol{R}_B) = \mathbf{dist}_\theta(\boldsymbol{R}_C\boldsymbol{R}_A, \boldsymbol{R}_C\boldsymbol{R}_B) = \mathbf{dist}_\theta(\boldsymbol{R}_A\boldsymbol{R}_C, \boldsymbol{R}_B\boldsymbol{R}_C) \tag{4.19}$$

4.4.3 Chordal distance in SO(3)

While the angular distance is a geodesic distance, in some applications it is more convenient to use a simpler expression for the distance, which often makes computation and analysis easier. Therefore we define the *chordal distance* between two rotations $\boldsymbol{R}_A \in \mathrm{SO}(3)$ and $\boldsymbol{R}_B \in \mathrm{SO}(3)$ as:

$$\mathbf{dist}_c(\boldsymbol{R}_A, \boldsymbol{R}_B) = \|\boldsymbol{R}_A - \boldsymbol{R}_B\|_F = \|\boldsymbol{R}_B - \boldsymbol{R}_A\|_F \tag{4.20}$$

where $\|\cdot\|_F$ is the *Frobenius* norm, which for a matrix $\boldsymbol{M}$ is defined as

$$\|\boldsymbol{M}\|_F = \sqrt{\sum_{ij} \boldsymbol{M}_{ij}^2} = \|\mathrm{vec}(\boldsymbol{M})\| = \sqrt{\sum_i \|\boldsymbol{M}_{i,:}\|^2} = \sqrt{\sum_j \|\boldsymbol{M}_{:,j}\|^2} = \sqrt{\mathrm{tr}\left(\boldsymbol{M}\boldsymbol{M}^\mathsf{T}\right)} \tag{4.21}$$

Fig. 4.2 sheds some light on the nature of the chordal distance.

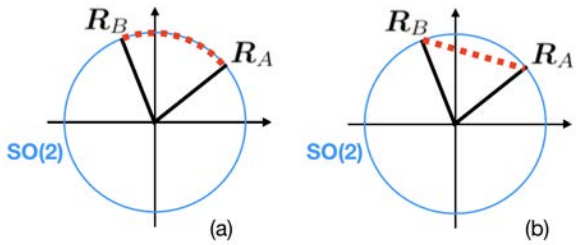

Figure 4.2: (a) Angular and (b) chordal distance in SO(2).

We can also relate the chordal distance to the angular distance for 3D rotations as follows:

$$\mathbf{dist}_c(\boldsymbol{R}_A, \boldsymbol{R}_B) = \|\boldsymbol{R}_A - \boldsymbol{R}_B\|_F = \|\boldsymbol{R}_B - \boldsymbol{R}_A\|_F = \sqrt{\mathrm{tr}\left((\boldsymbol{R}_B - \boldsymbol{R}_A)(\boldsymbol{R}_B^\mathsf{T} - \boldsymbol{R}_A^\mathsf{T})\right)} \tag{4.22}$$

$$\sqrt{\mathrm{tr}\left(2\mathbf{I}\right) - 2\mathrm{tr}\left(\boldsymbol{R}_A^\mathsf{T}\boldsymbol{R}_B\right)} = \sqrt{6 - 2(1 + 2\cos(\theta))} = 2\sqrt{1 - \cos(\theta)} \tag{4.23}$$

now recalling that $\sin^2(\theta/2) = \frac{1}{2}(1 - \cos(\theta))$:

$$\mathbf{dist}_c(\boldsymbol{R}_A, \boldsymbol{R}_B) = 2\sqrt{1 - \cos(\theta)} = 2\sqrt{2\sin^2(\theta/2)} = 2\sqrt{2}|\sin(\theta/2)| \tag{4.24}$$

which also holds for the 2D case [2] (which considers squared distances). Note that for small angles θ, $\sin(\theta/2) \approx \theta/2$ and:

$$\mathbf{dist}_c(\boldsymbol{R}_A, \boldsymbol{R}_B) \approx \sqrt{2}\,\mathbf{dist}_\theta(\boldsymbol{R}_A, \boldsymbol{R}_B) \tag{4.25}$$

Bi-invariance: for 3 rotations $\boldsymbol{R}_A, \boldsymbol{R}_B, \boldsymbol{R}_C$:

$$\mathbf{dist}_c(\boldsymbol{R}_A, \boldsymbol{R}_B) = \mathbf{dist}_c(\boldsymbol{R}_C\boldsymbol{R}_A, \boldsymbol{R}_C\boldsymbol{R}_B) = \mathbf{dist}_c(\boldsymbol{R}_A\boldsymbol{R}_C, \boldsymbol{R}_B\boldsymbol{R}_C) \tag{4.26}$$

4.4.4 Quaternion distance

When the two rotations are given as unit quaternions $\boldsymbol{q}_A$ and $\boldsymbol{q}_B$ one can compute the distance between them using the quaternion distance:

$$\mathbf{dist}_q(\boldsymbol{q}_A, \boldsymbol{q}_B) = \|\boldsymbol{q}_A - \boldsymbol{q}_B\| = \|\boldsymbol{q}_B - \boldsymbol{q}_A\| \tag{4.27}$$

This distance has been used in several works in the literature. Unfortunately, the distance above has a number of shortcomings. For instance, we know that $\boldsymbol{q}_B$ and $-\boldsymbol{q}_B$ represent the same rotation, however in general:

$$\mathbf{dist}_q(\boldsymbol{q}_A, \boldsymbol{q}_B) \neq \mathbf{dist}_q(\boldsymbol{q}_A, -\boldsymbol{q}_B) \tag{4.28}$$

This problem can be alleviated by redefining the quaternion distance as follows [3]:

$$\mathbf{dist}_q(\boldsymbol{q}_A, \boldsymbol{q}_B) = \min_{b \in \{-1;+1\}} \|\boldsymbol{q}_A - b\,\boldsymbol{q}_B\| \tag{4.29}$$

which however has the drawback of including a binary variable, which typically makes computation and analysis trickier.

4.4.5 Distances between poses

An excellent survey and discussion about distances in SE(3) is given in [5]. We remark that the metrics below "mix" angular quantities (radians) with Euclidean quantities (meters), hence typically there is some weighting factor that makes the quantities dimensionless.

4.4.6 Double Geodesic distance in SE(3)

Given two poses $\boldsymbol{T}_A \doteq (\boldsymbol{R}_A, \boldsymbol{t}_A)$ and $\boldsymbol{T}_B \doteq (\boldsymbol{R}_B, \boldsymbol{t}_B)$ a straightforward way to generalize (4.18) to SE(3) is:

$$\mathbf{dist}_g(\boldsymbol{T}_A, \boldsymbol{T}_B) = \|\log(\boldsymbol{T}_A^{-1}\boldsymbol{T}_B)^\vee\| = \|\log(\boldsymbol{T}_B^{-1}\boldsymbol{T}_A)^\vee\| \tag{4.30}$$

In the robotics literature, however, authors prefer to use the *double geodesic* distance between the two poses, which is defined as:

$$\mathbf{dist}_{dg}(\boldsymbol{T}_A, \boldsymbol{T}_B) = \sqrt{\| \log(\boldsymbol{R}_A^\mathsf{T} \boldsymbol{R}_B) \|^2 + \| \boldsymbol{t}_B - \boldsymbol{t}_A \|^2} = \sqrt{\mathbf{dist}_\theta(\boldsymbol{T}_A, \boldsymbol{T}_B)^2 + \| \boldsymbol{t}_B - \boldsymbol{t}_A \|^2} \tag{4.31}$$

which simply treats SE(3) as the Cartesian product of SO(3) and $\mathbb{R}^3$.

Left-invariance: for 3 poses $\boldsymbol{T}_A, \boldsymbol{T}_B, \boldsymbol{T}_C$:

$$\mathbf{dist}_g(\boldsymbol{T}_A, \boldsymbol{T}_B) = \mathbf{dist}_g(\boldsymbol{T}_C \boldsymbol{T}_A, \boldsymbol{T}_C \boldsymbol{T}_B) \tag{4.32}$$
$$\mathbf{dist}_{dg}(\boldsymbol{T}_A, \boldsymbol{T}_B) = \mathbf{dist}_{dg}(\boldsymbol{T}_C \boldsymbol{T}_A, \boldsymbol{T}_C \boldsymbol{T}_B) \tag{4.33}$$

4.4.7 Chordal distance in SE(3)

We define the *chordal distance* between two poses (in homogeneous coordinates) $\boldsymbol{T}_A \in \mathrm{SE}(3)$ and $\boldsymbol{T}_B \in \mathrm{SE}(3)$ as:

$$\mathbf{dist}_c(\boldsymbol{T}_A, \boldsymbol{T}_B) = \| \boldsymbol{T}_A - \boldsymbol{T}_B \|_F = \| \boldsymbol{T}_B - \boldsymbol{T}_A \|_F \tag{4.34}$$

It is easy to prove by inspection that:

$$\mathbf{dist}_c(\boldsymbol{T}_A, \boldsymbol{T}_B) = \sqrt{\mathbf{dist}_c(\boldsymbol{R}_A, \boldsymbol{R}_B)^2 + \| \boldsymbol{t}_B - \boldsymbol{t}_A \|^2} \tag{4.35}$$

Left-invariance: for 3 poses $\boldsymbol{T}_A, \boldsymbol{T}_B, \boldsymbol{T}_C$:

$$\mathbf{dist}_c(\boldsymbol{T}_A, \boldsymbol{T}_B) = \mathbf{dist}_c(\boldsymbol{T}_C \boldsymbol{T}_A, \boldsymbol{T}_C \boldsymbol{T}_B) \tag{4.36}$$

References

[1] T. Barfoot. *State Estimation for Robotics*. Cambridge University Press, 2017.

[2] L. Carlone and F. Dellaert. Duality-based verification techniques for 2D SLAM. In *IEEE Intl. Conf. on Robotics and Automation (ICRA)*, pages 4589–4596, 2015. (pdf) (code).

[3] L. Carlone, R. Tron, K. Daniilidis, and F. Dellaert. Initialization techniques for 3D SLAM: a survey on rotation estimation and its use in pose graph optimization. In *IEEE Intl. Conf. on Robotics and Automation (ICRA)*, pages 4597–4604, 2015. (pdf) (code) (supplemental material: (pdf)).

[4] G. S. Chirikjian. *Stochastic Models, Information Theory, and Lie Groups, Volume 2: Analytic Methods and Modern Applications (Applied and Numerical Harmonic Analysis)*. Birkhauser, 2012.

[5] G.S. Chirikjian. Partial bi-invariance of SE(3) metrics. *J. Comput. Inf. Sci. Eng*, 15(1):185–200, 2015.

[6] R. Hartley, J. Trumpf, Y. Dai, and H. Li. Rotation averaging. *IJCV*, 103(3):267–305, 2013.

[7] Y. Wang and G.S. Chirikjian. Error propagation on the euclidean group with applications to manipulator kinematics. *IEEE Trans. Robotics*, 22(4):591–602, 2006.

16.485 Visual Navigation for Autonomous Vehicles (VNAV)
Fall 2020